MICROSCALE PIERCED SHALLOW SHELL RESONATORS: A TEST VEHICLE TO STUDY SURFACE LOSS

Benoit Hamelin, Vahid Tavassoli, and Farrokh Ayazi
Georgia Institute of Technology, Atlanta, GA, USA

ABSTRACT

This paper reports on various energy dissipation mechanisms that limit the quality factor (Q) of micro-scale pierced shallow shell resonators (PSSRs). While low-frequency thick-film shells (t>50µm) exhibit Qs in excess of 1M, thin-film shells (t<5µm) of same frequency have so far failed to do so. PSSRs are ideal test vehicles to study the contribution of surface loss to the overall energy damping of thin-film shells. Optical measurements confirm mode confinement that stems from curvature discontinuities, which efficiently decouple the resonating rim from the dissipative anchor, and suppress anchor loss. Surface loss is found to be the main dominant damping mechanism of trapped modes in 2.6µm thick SiO_2 and TEOS PSSRs. We compare TEOS and thermally-grown SiO_2 (hereinafter referred to as SiO_2) as structural materials for high Q resonators and extract surface loss parameters for both. Quality factors as high as 111,000 have been measured, which corresponds to a 30% improvement to the state-of-the-art thin-film SiO_2 resonators.

INTRODUCTION

Recent efforts to develop chip-scale inertial measurement units (IMUs) have led to the miniaturization of the hemispherical resonating gyroscope (HRG) [1-12]. Low-frequency operation (3kHz<f<30kHz) in a compact form factor as well as suppression of support loss are some of the benefits that stem from migrating from planar to curved resonant structures [13]. These miniaturization efforts have developed new 3D micro-fabrication techniques to conserve the benefits of the curved structure of the HRG. These novel techniques fall into two main categories: Reshaping of thick-film wafers (thickness t >50µm), e.g. via blow torching [9-10], and deposition of thin films (t <5µm) into symmetric molds, usually etched in silicon (Si) substrates [1-8]. Although resonant gyroscopes fabricated using the former approach yield high mechanical quality factors (Q-factor) in excess of 1M, they are bulky (volume V=52mm^3 [10]) and not suited for integration in silicon. Unlike thick-film shells, the Q-factor of thin-film shells of similar frequency has so far failed to reach 1M. For instance, typical fabricated polysilicon thin-film (t=700nm) shells integrated in a silicon chip with self-aligned and scalable electrodes, defined using the 3D HARPSS process, provide rate measurement in a small form factor (V=0.86mm^3) [5]. Although highly desirable, the wide-spread use of thin-film shells for on-chip inertial navigation sensing is currently limited by their relatively lower Q values. Polysilicon µHRGs, with optimized anchoring pedestals, exhibit Q values as high as 40,000 at 11kHz [5]. Polysilicon has been replaced by thermally grown silicon dioxide (hereinafter SiO_2) to suppress the contribution of thermoelastic damping to the Q-factor.

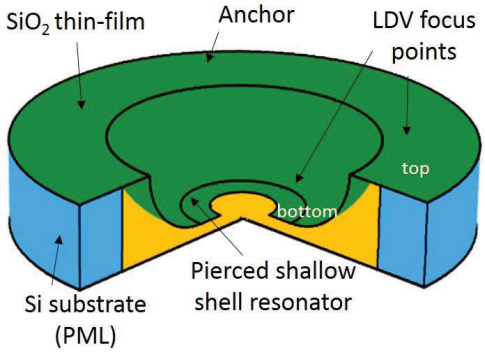

Figure 1: Schematic of a SiO_2 pierced shallow shell resonator (PSSR), anchored at the top surface.

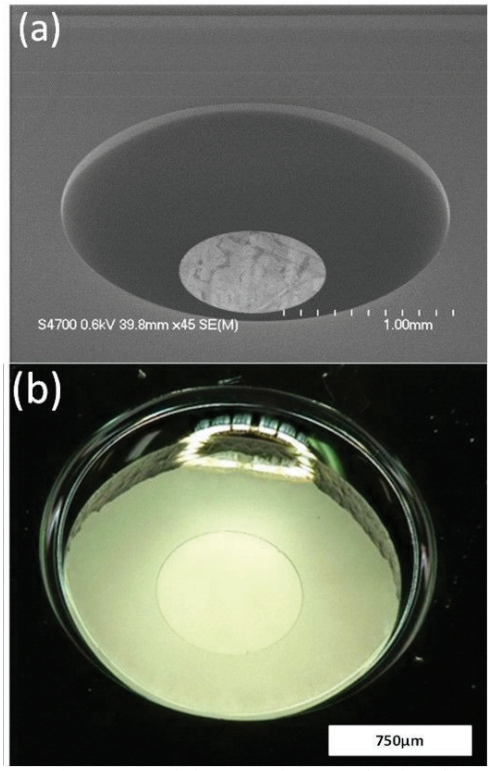

Figure 2: (a) SEM and (b) optical views of a thin-film SiO_2 pierced shallow shell resonator (PSSR).

In this paper, we introduce Pierced Shallow Shell Resonators (PSSRs) (Figures 1, 2) as simple test vehicles to study surface loss in various thin-films. We provide experimental evidence that anchor loss in certain trapped modes of PSSR is substanitally suppressed, making the Q to be bound by surface loss.

ENERGY LOSS MECHANISMS

While thick-film μHRGs exhibit high Q values as-expected by Finite Element Method (FEM) simulations, there is a large discrepancy between measured Q-factors and simulated Q-factors for low-stiffness shells, regardless of the choice of the investigated structural material (ALD alumina [1], CVD microcrystalline diamond [2, 3], poly-Si [5], SiO_2 [6-8]). The main independent dissipation mechanisms that limit the Q-factor (Q_{TOTAL}) of thin-film mechanical resonators are viscous damping including squeeze film damping (Q_{AIR}), thermoelastic damping (Q_{TED}), support loss (Q_{ANCHOR}), surface loss ($Q_{SURFACE}$) and Akhiezer damping (Q_{AKE}) as shown in (1).

$$\frac{1}{Q_{TOTAL}} = \frac{1}{Q_{AIR}} + \frac{1}{Q_{ANCHOR}} + \frac{1}{Q_{SURFACE}} + \frac{1}{Q_{TED}} + \frac{1}{Q_{AKE}} \quad (1)$$

The major result of this paper is to provide experimental evidence supporting that surface loss is the main dissipation mechanism that limits the Q-factor of thin-film shells resonating in the low frequency range.

Viscous damping is eliminated by operating low-frequency resonators at low vacuum levels, typically in the 100s of μTorr regime or below. The small coefficient of thermal expansion (CTE) of SiO_2 combined with the anti-biaxial strain state of hemispherical shells [14] enable bulk thermoelastic losses to be in excess of 1M. Furthermore, the small Poisson's ratio (σ=0.17) of SiO_2 combined with the large wavelength of smooth resonators (R_a=3.9nm on a 0.25μm^2 surface) limit the contribution of acoustic scattering due to roughness to the internal energy dissipation [15]. Surface roughness is however critical at the rim of the shell where bending in one direction is not compensated by bending in the normal direction, which induces a dissipative thermal gradient across the shell thickness. Therefore, the measured Q-factors are a combination of support loss and surface loss. Unfortunately, both surface loss and support loss in the low frequency operation range are challenging to simulate numerically. Surface loss results from the degradation of the surface layer of bulk films due to multiple mechanisms, including micro-cracks, adsorbed gas and water molecules [16]. This variety of mechanisms limits the development of numerical models of surface loss. Support loss is commonly simulated by using the perfectly matched layer (PML) method, method which is numerically extensive for resonators in the low frequency range due to their relatively large wavelength. Alternative methods to estimate support loss have been proposed but do not account for the large discrepancy between simulated and measured Q values for low-frequency resonators [17].

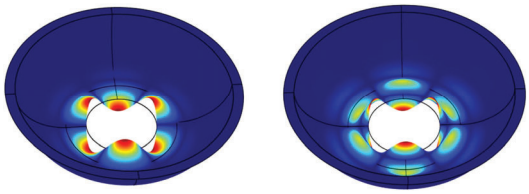

Figure 3: Trapped-mode families (left) secondary out-of-plane elliptical (3,0) mode and (right) higher order (3,1) mode.

PIERCED SHALLOW SHELL RESONATOR

In this paper, we investigate the resonant modes of PSSRs in the lower end of the mid-frequency range (30kHz<f<30MHz) to be able to simulate the exact value of $Q_{SUPPORT}$ using the conventional PML method in COMSOL 5.1. The modes below 500kHz that are confined at the bottom of PSSRs belong to two sets referenced in Figure 3 by (n,m), with 2n antinodes in the polar (θ) direction, and m+1 antinodes in the azimuthal (ϕ) direction where m=0 or m=1. The (n,0) elliptical out-of-plane modes are the modes of interest in this work, and the (n,1) modes are a set of higher harmonics. Surface loss parameters calculated for mid-frequency modes can be used to estimate the limiting energy dissipation factor of low-frequency gyroscopic modes (Figure 4).

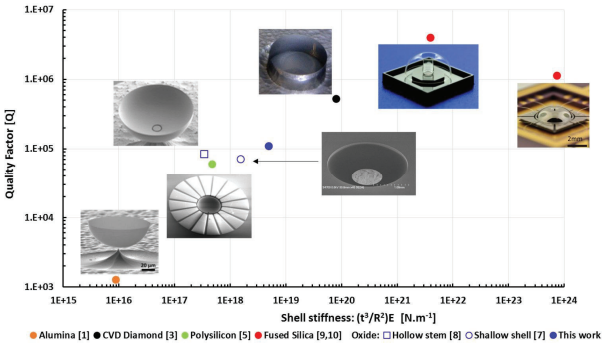

Figure 4: Q factors of low-frequency shells scale with the shell stiffness, which is proportional to the product (t^3/R^2)E, where t is the shell average thickness, R is the shell largest radius and E is the Young's modulus.

Traditionally, pedestal-supported shells are anchored at the bottom where the presence of the antinodes of coupled gyroscopic elliptical modes decouples the resonator from the dissipative substrate [18]. To further enhance decoupling, various approaches have been explored including reducing the dimensions of the pedestal to below 1μm [1], cutting slots using Focused Ion Beam (FIB) [2], or by making the anchoring pedestal tall and hollow [8,17]. These substrate-decoupling approaches require costly advanced fabrication techniques. In addition, the robustness of these shells to shock and vibrations might be degraded due to the extremely small dimensions of the anchoring pedestals. An alternative cost-effective substrate-decoupling approach introduces points of critical curvature in the shell to produce a transition region between the resonating rim and the dissipative substrate [7]. While in this paper the structure of PSSRs are identical to the resonator introduced in [7], the pedestal at the bottom is removed and the shell is anchored at the top. This anchoring approach provides PSSRs that are embedded in the Si substrate, with excellent handling capabilities, which improves fabrication yield without degrading Q_{ANCHOR}.

Laser Doppler Vibrometry (LDV, Polytec Inc.) velocity measurements at the anchor at the top of vibrating shells do not reveal observable peaks for the (3,0) mode. The absence of measurable peak is in good agreement with

numerical simulations that predict $Q_{ANCHOR} = 17M$ and negligible displacement (Figure 5). The measurement of 11 shells, with different anchor dimensions, provide statistical evidence that the distribution of the Q-factor of the (3,0) mode has higher mean and smaller standard deviation than the (1,0) and (2,0) modes (Figure 6). Because of energy confinement, the (3,0) and (10,0) modes are trapped at the bottom of the PSSR, contrary to the (1,0) and (2,0) modes. The simulated Q_{ANCHOR} of the (10,0) mode is in excess of the fundamental limit set by TED and Akhiezer dampings ($Q_{AKE+TED} \cong 500{,}000$). Figure 7 reveals that PML simulations predict that both Q_{TED} and Q_{ANCHOR} are orders of magnitude larger than $Q_{MEASURED}$, while the Q-factor distribution converges to about 94,000 for the ($3 \leq n \leq 11,0$) mode. A converging distribution indicates that surface loss, which is frequency independent (see Equation 2), might be the limiting factor of the ($n \geq 3,0$) elliptical modes.

SURFACE LOSS-LIMITED SHELLS

There is a general trend among the published μHRG work of increasing Q-factor with increasing stiffness (Figure 4). Therefore, energy dissipation mechanisms, such as surface loss that are controlled by stiffness, are good candidates as the mechanism that limits the Q-factor of low-stiffness shells. For resonators of thickness t, of width w>>t and of Young's modulus E covered by a dissipative coating layer of thickness δ and loss modulus E_{ds}, a standard model of surface loss is given by (2) [19].

$$Q_{SURFACE} = \frac{tE}{6\delta E_{ds}} \qquad (2)$$

To validate that surface loss is the limiting loss factor of the modes of interest, we have tested multiple PSSRs of identical dimensions with different structural materials,

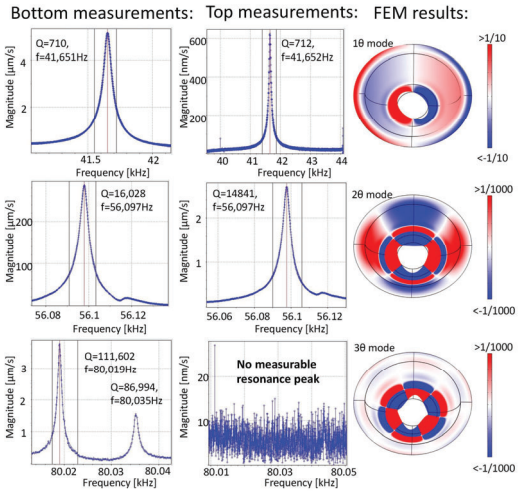

Figure 5: Laser Doppler Vibrometry (LDV) measurements reveal over a 1/100th reduction of the out-of-plane (OOP) displacement w of the (3,0) elliptical mode between (left) the resonating bottom and (center) the dissipative top of PSSRs, proving energy confinement of the (3,0) mode. Finite element simulations (right) confirm the LDV measurements. Top and bottom in PSSRs are defined in Figure 1.

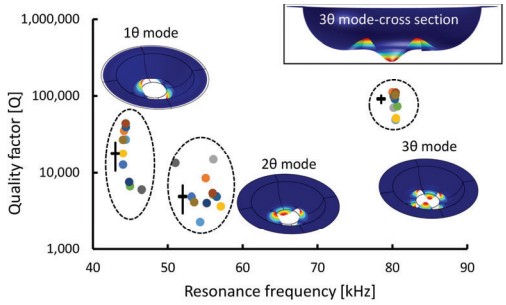

Figure 6: The narrow distribution of the Q-factors of 11 measured shells reveals that the (3,0) mode is statistically not support-loss limited. The cross indicates the mean and the standard deviation.

including thermal SiO_2 and thermally annealed SiO_2 deposited in a LPCVD-TEOS furnace (hereinafter TEOS). The etch rates of TEOS and SiO_2 by XeF_2 are nearly identical, providing evidence that TEOS after annealing is as dense as SiO_2 (Figure 8 b). The Q-factor of the (3,0) mode of 11 SiO_2 shells and 24 structurally similar TEOS shells have been measured. In average, the Q-factor of the substrate-decoupled (3,0) mode is doubled in SiO_2 shells compared to TEOS shells. Smoother SiO_2 shells published in previous work have lower Q-factors [6-8] than the SiO_2 PSSRs measured in this work. Although rougher than SiO_2 PSSRs, TEOS PSSRs may have lower Q-factors because of hydrocarbons (e.g. CO_2, CH_4) or voids that remain trapped in the TEOS film, even after exposing TEOS to a high temperature annealing step ($T_{annealing}$=1100°C) [20].

While a record high Q=111,000 has been measured for the (3,0) mode in a SiO_2 PSSR (Figure 8 c), the average Q-factor obtained from 11 shells is Q=92,000, in good agreement with Q=94,000, which is the Q-factor averaged out of 8 higher order substrate-decoupled modes in a single PSSR (Figure 7). By combining (1) and (2), we can extract from the LDV measurements that δE_{ds}=0.31N.m^{-1} for SiO_2 and δE_{ds}=0.61N.m^{-1} for annealed TEOS. Compared to SiO_2,

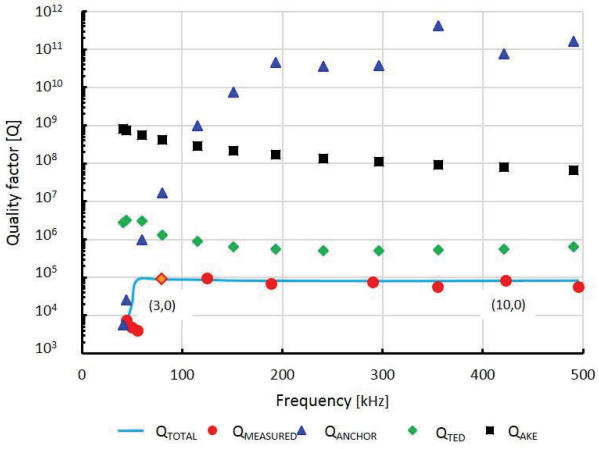

Figure 7: Q factor distribution of the family of resonant modes ($n \geq 0,0$) in a single PSSR. The (3,0) mode (orange diamond dot) is the lowest mode in frequency to be surface loss-limited. The value $Q_{SURFACE}$=94,000 best fits the Q-distribution of the ($n \geq 3,0$) modes. Q_{TOTAL} is defined in (1).

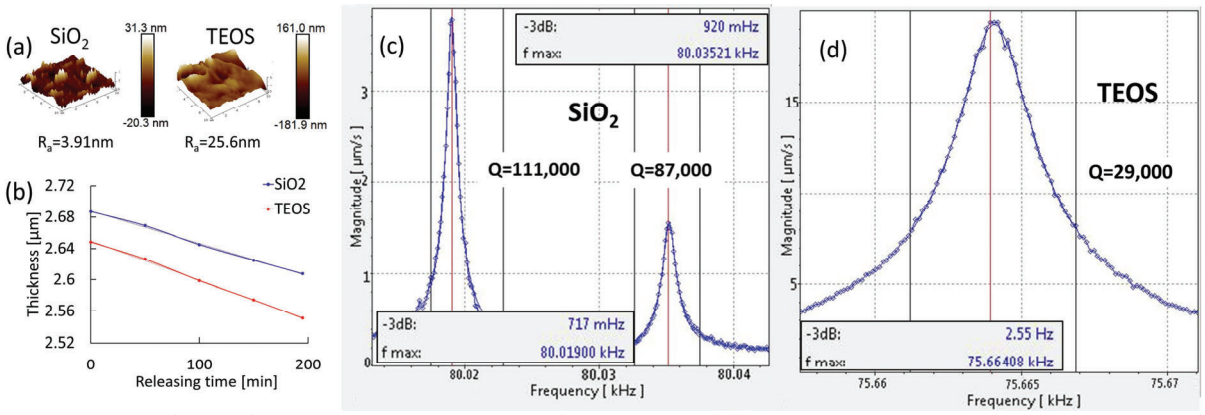

Figure 8: The quality factor of the (3,0) mode in PSSRs is surface-loss limited. While (a) roughness and (b) etch rate in XeF_2 of SiO_2 and TEOS are similar, the Q-factor of (c) the (3,0) mode in SiO_2 PSSRs is systematically greater than in (d)TEOS PSSRs.

microcrystalline CVD diamond has larger δE_{ds} parameters regardless of annealing conditions as well as larger Young's modulus [2], which results in smaller surface loss effects in microcrystalline CVD diamond compared to SiO_2 according to (2). Finally, the trapped (10,0) resonant mode provides the highest f.Q=3.58E10 product for thin-film SiO_2 shells (Figure 9).

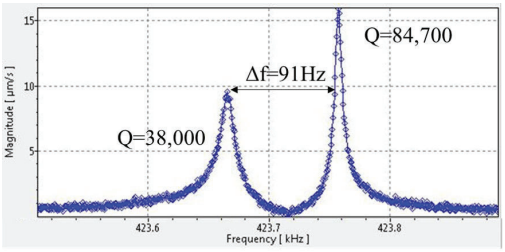

Figure 9: Highest f.Q=3.58E10 measured for SiO_2 resonators

CONCLUSION

Pierced shallow shell resonators have been presented as test vehicles to isolate and measure surface loss of thin-film resonators deposited on atomically-smooth Si molds. Using thermal silicon dioxide and LPCVD TEOS as structural materials revealed that out-of-plane elliptical modes of order n≥3 have negligible support and thermoelastic losses and are limited by surface effects. The highest measured Q=111,000 and highest f.Q=3.6E10 for thin-film thermal SiO_2 resonators are reported. The f.Q product is still about 10 times below the fundamental limit set both by thermoelastic and Akhiezer losses.

ACKNOWLEDGEMENTS

The DARPA Microsystems Technology Office, Microscale Rate Integrating Gyroscope (MRIG) program supported this work.

REFERENCES

[1] J. Gray, et al., "Hemispherical micro-resonators from atomic layer deposition," *J. Micromech. Microeng.*, **24**, (12), 1, 2014.

[2] J. Bernstein, et al., "High Q diamond hemispherical resonators: fabrication and energy loss mechanisms," *J. Micromech. Microeng.*, **25**, 1, 2015.

3] D. Saito, et al., "Microcrystalline diamond cylindrical resonators with quality-factor up to 0.5 million", *Appl. Phys. Lett.*, **108**, 2016.

[4] N. Mehanathan, et al., "Invar-36 micro hemispherical shell resonators," in *IEEE MEMS*, San Francisco, CA, 2014, pp. 40–43.

[5] P. Shao, et al., "A 3D-HARPSS polysilicon microhemispherical shell resonating gyroscope: Design, fabrication, and characterization," *IEEE Sensors J.*, **15**, (9), 4974, 2015.

[6] P. Shao, et al. "Electrical characterization of ALD-coated silicon dioxide micro-hemispherical shell resonators," *2014 IEEE 27th International Conference on Micro Electro Mechanical Systems (MEMS)*, San Francisco, CA, 2014, pp. 612-615.

[7] B. Hamelin, et al., "Highly-symmetric silicon dioxide shallow shell resonators with angstrom-level roughness," *SENSORS, 2015 IEEE*, Busan, 2015, pp. 1-4.

[8] V. Tavassoli, et al., "Substrate-Decoupled 3D Micro-Shell Resonators," *SENSORS, 2016 IEEE*, Orlando, 2016, pp. 1-4.

[9] D. Senkal, et al., "Demonstration of 1 million Q-factor on micro-glassblown wineglass resonators with out-of-plane electrostatic transduction," *J. Microelectromech. Syst.*, **24**, 29, 2015.

[10] J. Cho, et al., "130 second ring-down time and 3.98 million quality factor in 10 kHz fused silica micro birdbath shell resonator" in *Solid-State Sensors, Actuators and Microsystem Workshop*, 2016, pp. 408-411.

[11] L. Sorenson, et al. "3-D micromachined hemispherical shell resonators with integrated capacitive transducers," *Micro Electro Mechanical Systems, 2012 IEEE 25th International Conference on*, Paris, 2012, pp. 168-171.

[12] F. Ayazi, "Multi-DOF Inertial MEMS: From Gaming to Dead Reckoning," *Invited Paper*, *Tech. Digest of the 16th International Conference on Solid-State Sensors, Actuators and Microsystems* (*TRANSDUCERS'11*), Beijing, 2011, pp. 2805.

[13] D. Rozelle, The hemispherical resonator gyro: from wineglass to the planets, in: *Proc. AAS/AIAA Space Flight Mechanics Meeting*, 2009, pp. 1157-1178.

[14] L. Sorenson, P. Shao and F. Ayazi, "Bulk and Surface Thermoelastic Dissipation in Micro-Hemispherical Shell Resonators," *J. of Microelectromech. Syst.*, **24**, (2), 486, 2015.

[15] B. Shiari and K. Najafi, "Surface effect influence on the quality factor of microresonators," *2013 Transducers & Eurosensors XXVII: The 17th International Conference on Solid-State Sensors, Actuators and Microsystems (TRANSDUCERS & EUROSENSORS XXVII)*, Barcelona, 2013, pp. 1715.

[16] V. Braginski, Systems with Small Dissipation, The University of the Chicago Press, 1985.

[17] L. Sorenson and F. Ayazi, "Effect of structural anisotropy on anchor loss mismatch and predicted case drift in future micro-Hemispherical Resonator Gyros," *2014 IEEE/ION Position, Location and Navigation Symposium, CA*, 2014, pp. 493-498.

[18] B. Hamelin, V. Tavassoli and F. Ayazi, "Localized Eutectic Trimming of Polysilicon Microhemispherical Resonating Gyroscopes," *IEEE Sensors Journal*, **14**, (10), 3498, 2014.

[19] K. Yasumura *et al.*, "Quality factors in micron- and submicron-thick cantilevers," *J. of Microelectromech. Syst.*, **9**, (1), 117, 2000.

[20] R. Zorich, Handbook of Quality Integrated Circuit Manufacturing, Academic Press, 1991

CONTACT

*B. Hamelin, bhamelin3@gatech.edu